**1.**

**LA-UR**-80-1167

$C \cdot C \ \mathcal{L} f - \mathcal{J} C \ C \mathcal{J} \ \mathcal{I} / . \ - \mathcal{L}$

TITLE:  FLUX AT A POINT IN MCNP

**MASTER**

AUTHOR(S):   E.D. Cashwell, X-6
             R.G. Schrandt, X-6

SUBMITTED TO:   Proceedings of Seminar on Theory and Applications
                of Monte Carlo Methods

**University of California**

# LOS ALAMOS SCIENTIFIC LABORATORY
Post Office Box 1663   Los Alamos, New Mexico 87545
An Affirmative Action/Equal Opportunity Employer

# FLUX AT A POINT IN MCNP

E. D. Cashwell and R. G. Schrandt
Group X-6
Monte Carlo, Applications and Transport Data Group
Theoretical Applications Division
Los Alamos Scientific Laboratory
Los Alamos, New Mexico

## ABSTRACT

The current state of the art of calculating flux at a point with MCNP is discussed. Various techniques are touched upon, but the main emphasis is on the fast improved version of the once-more-collided flux estimator, which has been modified to treat neutrons thermalized by the free gas model. The method is tested on several problems of interest and the results are presented.

## INTRODUCTION

The next-event estimator (NEE) used in a normal Monte Carlo game for the flux at a detector embedded in a scattering medium suffers from a $(1/r^2)$-singularity. Consequently, the variance of the estimator is infinite even though the mean is finite.

In 1977, Kalli and Cashwell[1] proposed and evaluated three estimation schemes for flux at a point. A new, once-more-collided flux estimator (OMCFE) was proposed, which differed from those proposed by Kalos in his original paper.[2] The scheme has a $(1/r)$-singularity, leading to finite variance and $(1/\sqrt{N})$-convergence. It is based on a very simple p.d.f. of the path lengths in the sampling of the intermediate collision points. In addition, this simple p.d.f. for the path length was used in two schemes with bounded estimators similar to those proposed by Steinberg and Kalos[3] and by Steinberg.[4] The three schemes were evaluated in a realistic problem using the continuous energy Los Alamos Monte Carlo code MCNG, the forerunner of MCNP.[5]

## Once-More Collided Flux Estimator (OMCFE)

In the present discussion we wish to focus on the OMCFE referred to above. This scheme has been incorporated into MCNP and, although some work still remains to be done, we wish to discuss this method in conjunction with other techniques available in MCNP.

The details of the OMCFE as it exists in MCNP are, for the most part, given in Ref. (1). Without repeating the treatment given there, we wish to touch on the main points of the method, as well as mention generalizations of the method to a wider class of problems. The OMCFE is superimposed on the particle history without affecting it. At each collision (or source point), a nonanalog game is played whereby a next collision point A is chosen, from which a contribution to the detector is made. That is, from every real collision point of the particle history, a once-more-collided contribution is made to the detector.

The two main features in determining the intermediate point A of the once-more-collided scheme are:

1. A directional reselection procedure based on the reselection technique of Steinberg and Kalos;[3] and

2. A nonanalog p.d.f. $p^*(s)$ which was used by Kalli[6] in 1972.

In Fig. 1, consider a collision at S with the resulting scattered direction $\vec{\Omega}_o$ in the cone described. Suppose that a new direction $\vec{\Omega}_1$ is chosen by sampling a new angle $\beta_1$ uniformly in $(0, \beta_m)$ and a $\phi_1$ uniformly in $(0, 2\pi)$. The result is a concentration of scattered directions closer to the line from S to the detector D than would normally occur. Of course, an adjustment factor must be applied to the weight of the particle due to the reselection.

Once the direction $\overline{\Omega}_1$ is chosen. suppose the intermediate point A is selected along this direction from the p d.f. $p^*(s)$, where

$$p^*(s) = \frac{b}{(\pi/2 - \alpha_1)r^2} \quad \text{(Cf. Fig. 2).} \tag{1}$$

This density function corresponds to $\alpha$ being chosen uniformly in $(\alpha_1, \pi/2)$. Use of $p^*(s)$ leads to another weight adjustment $p(s)/p^*(s)$, where $p(s)$ is the analog p.d.f. for sampling distance to collision.

In the normal OMCFE, the point A is not a real collision point of the particle history. When these calculations involve reselection of direction and the distance to A using $p^*(S)$, as well as the normal next-event estimator, they tend to be time-consuming. In order to speed up calculations using the OMCFE:

1. Draw an imaginary sphere around the detector;

2. If the collision point $S_1$ is outside the sphere but the direction after the collision is within the cone defined by $S_1$ and he sphere, calculate the once-more-collided flux contribution by performing the directional reselection in the cone and calculate the intermediate point A by using $p^*(s)$;
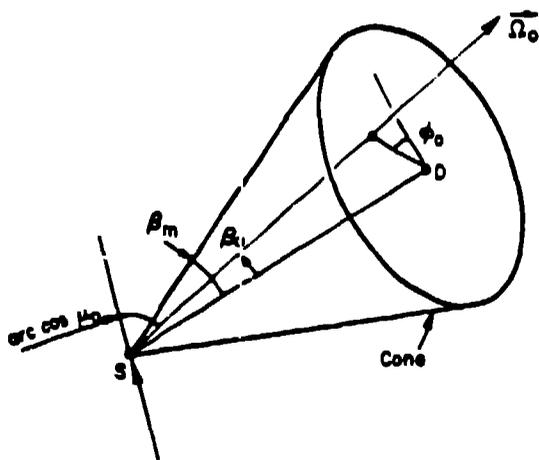
Fig. 1.  Geometry in the re-
selection of a  direction.
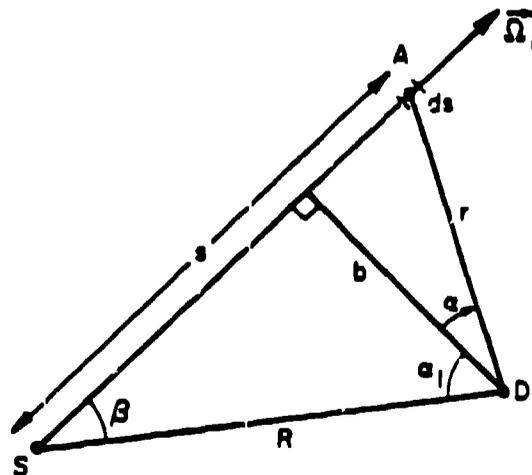
Fig. 2.  Geometry in the selec-
tion of the intermediate col-
lision point A.

3.  If the collision point $S_i$ is in the sphere and the direction $\vec{\Omega}_o$
after collision is in a ?--cone (i.e., $\beta_o < \pi/2$) about the line from $S_i$
to D, the once-more-collided point is calculated by reselection of $\vec{\Omega}_1$
and using $p^*(s)$ to determine the intermediate point A; if the direction
$\vec{\Omega}_o$ after collision is such that $\beta_o > \pi/2$, no reselection is performed
but the intermediate point A is chosen from $p^*(s)$; and

4.  Otherwise, calculate the normal next-event contribution from
the following collision point $S_{i+1}$.

The recipe as outlined above works very well in most problems
containing ordinary materials.  However, in non-thermal problems
containing H, the forward scattering off H in the laboratory system of
coordinates lead to some modification of the recipe because of the
directional reselection procedure.  Furthermore, the random motion of
the target atoms combined with the motion of the neutron in the thermal
routine using the free gas model in MCNP leads to rather extensive
modifications for the same reason.  The imaginary sphere around the
detector may have to be reduced in size in the course of the
calculation, as a result of using the reselection procedure.

With the necessary modifications, MCNP is able to treat problems of
the types mentioned above, as illustrated by the sample calculations
below.  Several considerations led to the implementation of the OMCFE
rather than one of the schemes leading to a bounded estimator in Ref.
(1).  First of all, the OMCFE was judged to be the simplest to insert
into MCNP.  Furthermore, the estimation of flux simultaneously at
several points causes no problems in the OMCFE scheme.  Finally, since
the OMCFE does not alter the particle histories, its use has no effect
on other tallies which may be required in a particular problem.

# DXTRAN

Let us describe briefly a subroutine, DXTRAN, which has been used in Los Alamos for some years and is an option available in MCNP.[5] We shall indicate its usefulness in our examples below. DXTRAN is of value in sampling regions of a problem which may be insufficiently visited by particle histories to yield adequate statistical accuracy in a given tally. To explain how the scheme works, let us consider the neighborhood of interest to be a spherical region surrounding a designated point $P_0$ in space. In fact, we consider two spheres of arbitrary radii about the point $P_0(x_0,y_0,z_0)$. We assume that the particle having direction $(u,v,w)$ collides at the point $(x,y,z)$, as shown in Fig. 3. The quantities $L$, $\theta_I$, $\theta_0$, $\eta_I$, $\eta_0$, $R_I$, and $R_0$ are clear from the figure. Let us somehow choose a point $P_s$ on the outer sphere and assume that a scattered particle (let us call it a "pseudo-particle" for the moment) is placed there. We give this pseudo-particle a weight equal to the weight of the incoming particle at $P_1$ multiplied by the ratio of the p.d.f. for scattering from $P_1$ to $P_s$ with no collision to the p.d.f. for choosing the point $P_s$ in the first place.

If we sample directions isotropically in the cone defined by $P_1$ and the outer sphere, the number of directions falling inside the inner cone and the number falling in the outer cone will be proportional to $1-\eta_I$ and $\eta_I-\eta_0$, respectively. Let Q be a factor which measures the weight or importance which one assigns to scattering in the inner cone relative to scattering in the outer cone. We now proceed by the following steps:
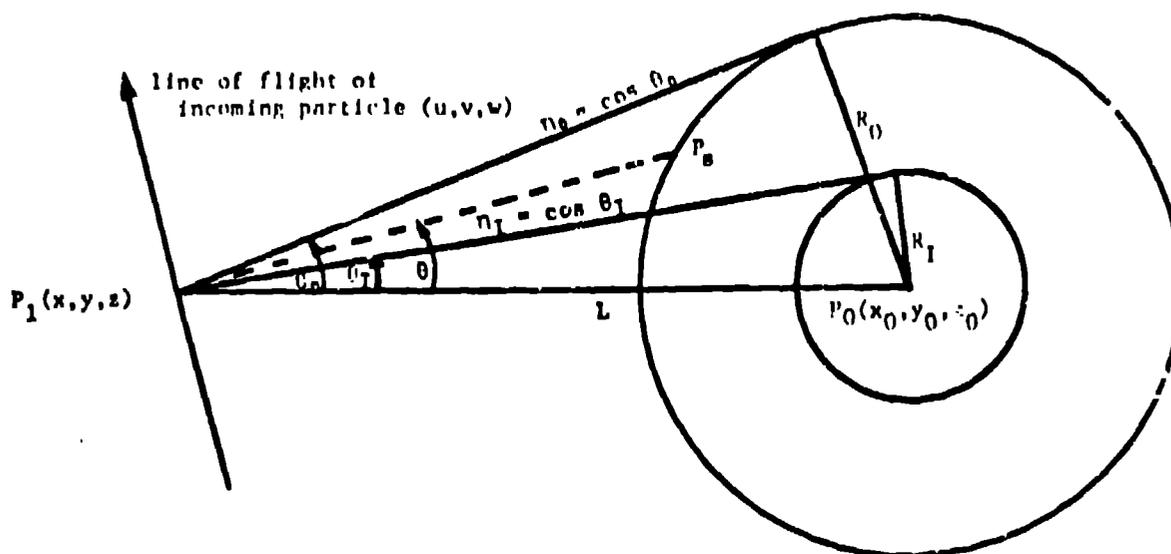


Fig. 3. The geometry of DXTRAN.

1.  Sample $\eta$ uniformly in $(\eta_I, 1)$ with probability $Q(1-\eta_I)/[Q(1-\eta_I) + \eta_I-\eta_0]$; and with probability $(\eta_I-\eta_0)/[Q(1-\eta_I) + \eta_I-\eta_0]$ sample $\eta$ uniformly in $(\eta_0, \eta_I)$;

2.  Having chosen $\theta$ from $\eta = \cos\theta$, we use the scattering formulas in the code to scatter through an angle $\theta$ (and an azimuthal angle $\phi$ chosen uniformly in $(0, 2\pi)$) from the initial direction $\left(\dfrac{x_o-x}{L}, \dfrac{y_o-y}{L}, \dfrac{z_o-z}{L}\right)$, determining a new direction $(u', v', w')$. Advance the pseudo-particle in the direction $(u', v', w')$ to the point $P_s$ on the surface of the outer sphere. The new coordinates are saved;

3.  The weight attached to the pseudo-particle is the weight of the particle at collision multiplied by

$$\nu \cdot \frac{P(\mu)\{Q(1 - \eta_I) + \eta_I - \eta_0\}\,\exp\left\{-\displaystyle\int_{P_1}^{P_s} \Sigma_t(s)\,ds\right\}}{Q}, \quad \eta_I < \eta < 1$$

and

$$\nu \cdot P(\mu)\{Q(1 - \eta_I) + \eta_I - \eta_0\}\,\exp\left\{-\displaystyle\int_{P_1}^{P_s} \Sigma_t(s)\,ds\right\}, \quad \eta_0 < \eta < \eta_I \quad ,$$

where

$\mu = uu' + vv' + ww'$

$P(\mu)$ = p.d.f. for scattering through the angle $\cos^{-1}\mu$ in the lab system for the event sampled at $(x,y,z)$.

$\nu$ = number of neutrons emitted from the event.

Since a collision supplies a particle (let us now drop the term pseudo-particle - these particles are as real as any others) to the outer DXTRAN sphere, the particles from the collision at $P_1$ are picked up and followed further, but they are killed if they attempt to enter the sphere. It is apparent from the discussion above that this routine has certain features in common with a point detector routine.

This routine is used in a couple of the problems discussed below. In one problem, it is used to obtain the average flux in a small volume as a check against the result obtained from the OMCFE. In another, it is used to help get particles in the vicinity of a detector. While DXTRAN can be useful in many problems, it must be pointed out that the method is time-consuming, being similar in nature to a point detector routine. Further, attention must be paid to the problem of obtaining a sufficient number of histories in the vicinity of the DXTRAN sphere, not just inside the sphere.

# CALCULATIONS

The problems discussed below were chosen to demonstrate the
behavior of the OMCFE in a variety of settings, with some emphasis on
the treatment of H and, in particular, its behavior in the presence of
neutrons thermalized according to the free gas model.  Illustrations of
how DXTRAN can be useful, either as an aid to the OMCFE or as an aid in
computing the average flux in a region with a track-length estimator,
occur in two of the problems.

The geometries displayed in our problems are deliberately kept
simple, partly so that we can display the so-called "exact flux", which
is calculated very accurately (to a fraction of a percent) using a
surface crossing estimator in the spherical geometry.  In the schematics
showing the geometry used, not every surface appears.  Frequently,
additional surfaces were added for the purposes of splitting and Russian
roulette, or for the purpose of obtaining average flux in a region, but
few surfaces were added in any one calculation.

In each problem, the source at the center of the sphere was chosen
to be monoenergetic and isotropic in direction.  As easily anticipated,
it was found useful to use an exponential biasing to direct more
particles toward the detectors.  The latter were always placed on a
radius of the sphere - say the positive x-axis.  The initial flight of a
neutron was chosen by sampling $\mu$ , the cosine of the angle the starting
direction makes with the x-axis, from a p.d.f. $\sim e^{k\mu}$, with k a fixed
parameter.  The value of k used in each problem is listed on the
schematic for that problem.

A feature of MCNP which was used in these calculations has to do
with contributions to the detector D from collisions several free paths
from the detector.  E.g., when collisions occur more than x free paths
from D, by playing Russian roulette one can permit, say, only one in ten
collisions on the average to contribute to D, with weight enhanced by a
factor of ten.  The number x is set by the user and in these
calculations was usually set to four.  This feature of the code can save
appreciable amounts of machine time in large systems.

Other information on the schematic which is of interest include the
number density of atoms in the material used; the thermal temperature of
the problem (if any); the average m.f.p. $\overline{\lambda}$ , computed by MCNP over the
course of the problem ; the source energy and energy cut-off (if any);
the time on the CDC-7600 for a given sample of starting neutrons; and
the imaginary sphere radii used in the OMCFE and in DXTRAN.

Figs. 4-12 display the geometries and graphs of the results for
four problems.  Table 1 gives a comparison of the final flux values at
the end of each run with the "exact values".  The errors in the final
fluxes also appear.

H

No. atoms/cm$^3$ = 0.025 × 10$^{24}$

Thermal temp. = 2.5 × 10$^{-8}$ MeV

$\bar{\lambda}$ ~ 1.6 cm

0    2.0   4.0     6.33 cm

Isotropic source at (0,0,0)

Energy = 4.0 × 10$^{-7}$ MeV

Exponentially biased toward

detectors, with k = 0.5

Detectors

OMC sphere radii

= 3.0 cm

Time – 15 min. for 100000 particles
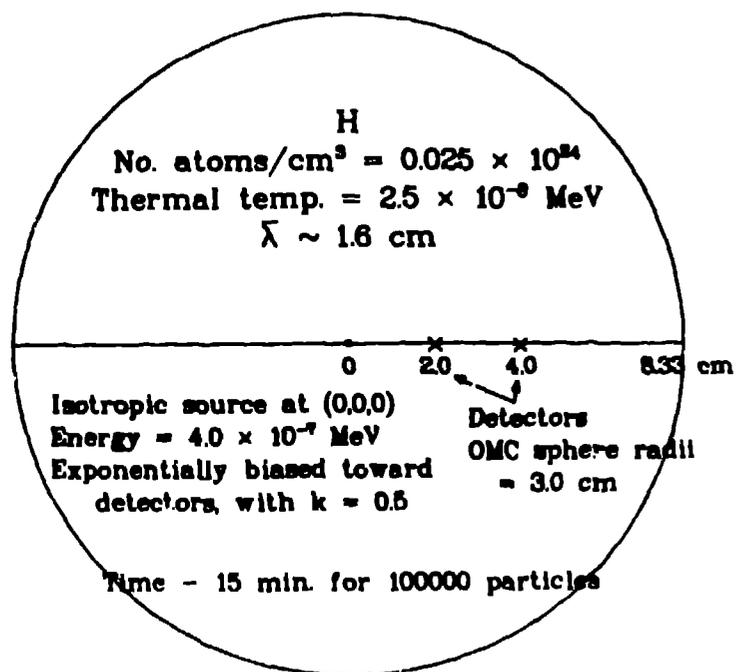
Fig. 4   Geometry for Thermal Hydrogen Problem.
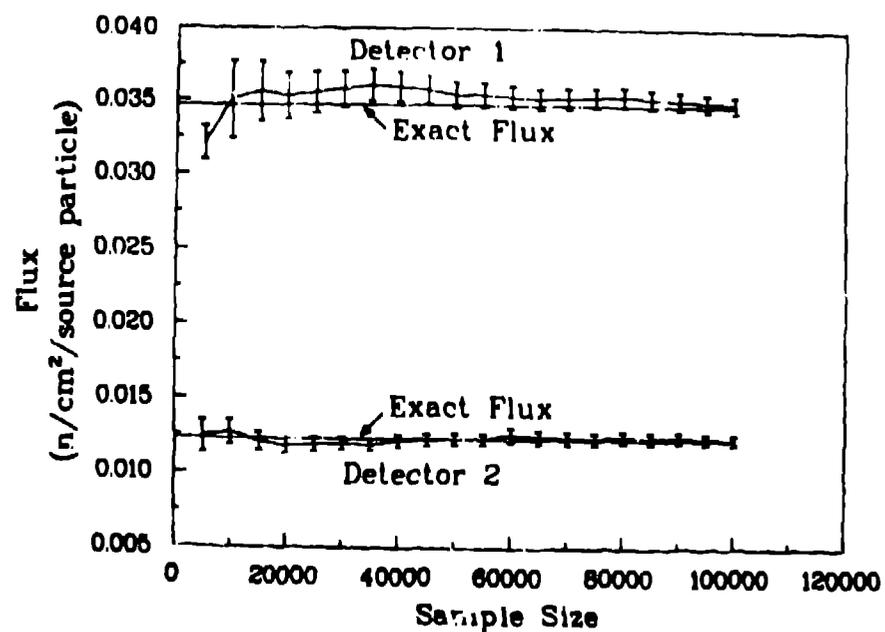


Fig. 5   Flux at Two Detectors in
Thermal H with the OMCFE.

CH$_2$
No. atoms/cm$^3$ = 0.118 × 10$^{84}$
Thermal temp. = 2.5 × 10$^{-8}$ Me$^v$
$\overline{\lambda}$ ~ 0.43 cm

0    1.0    2.0    3.0 cm

Isotropic source at (0,0,0)    Detectors
Energy = 4.0 × 10$^{-7}$ MeV    OMC sphere
Exponentially biased toward        radius = 0.9 cm
detectors, with k = 0.9
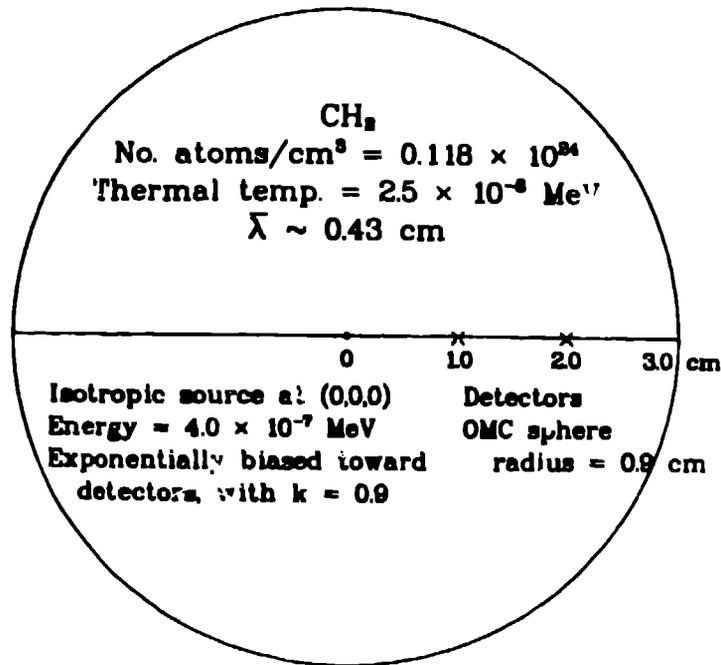
Fig. 6    Geometry for Thermal CH$_2$ Problem.
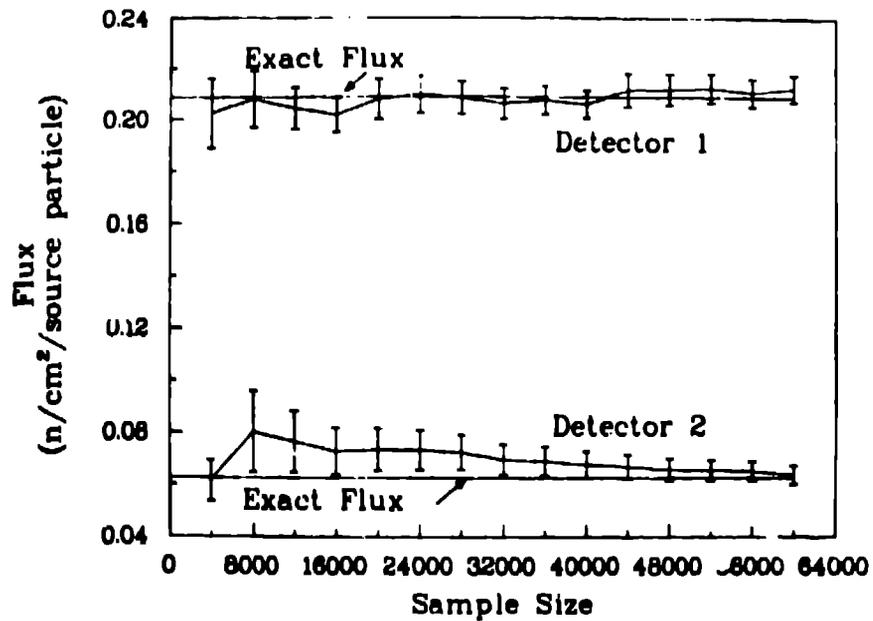


Fig. 7    Flux at Two Detectors in
Thermal CH$_2$ with the OMCFE.

BeO-1
No. atoms/cm$^3$ = 0.144 × 10$^{24}$
$\bar{\lambda}$ ~ 1.75 cm

0    3.5    8.0 cm

Isotropic source
Energy = 1.0 MeV
$E_{cutoff}$ = 0.1 MeV
Exponentially biased toward
detector, with k = 0.75

Detector
OMC sphere radius
= 2.0 cm
DXTRAN sphere radii
= 1.1, 2.0 cm

Time { OMCFE - 8.5 min. for 100000 particles
       DXTRAN - 5.7 min. for 15000 particles
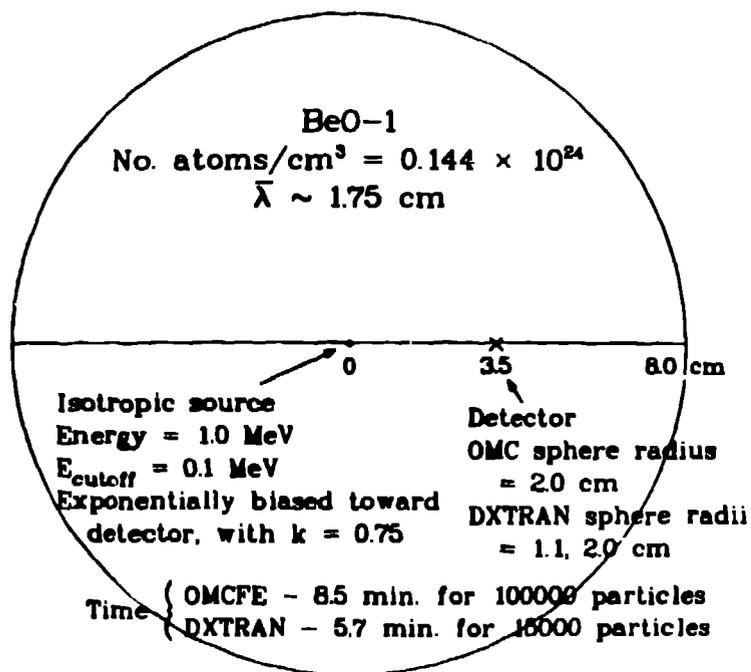
Fig. 8   Geometry for BeO-1 Problem.
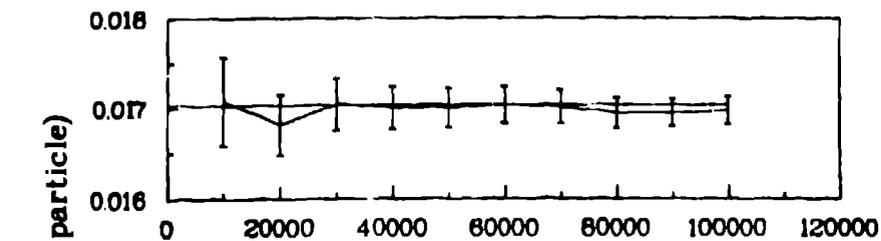


Fig. 9   Flux at a Detector in BeO-1
with the OMCFE.



Sample Size
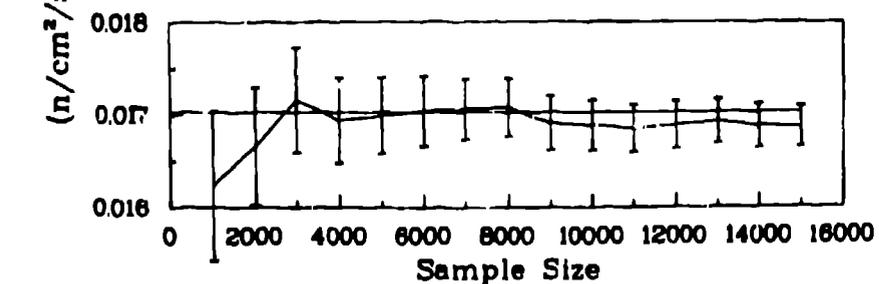
Fig. 10   Average Flux in the Vicinity
of a Detector in BeO-1 Using DXTRAN.
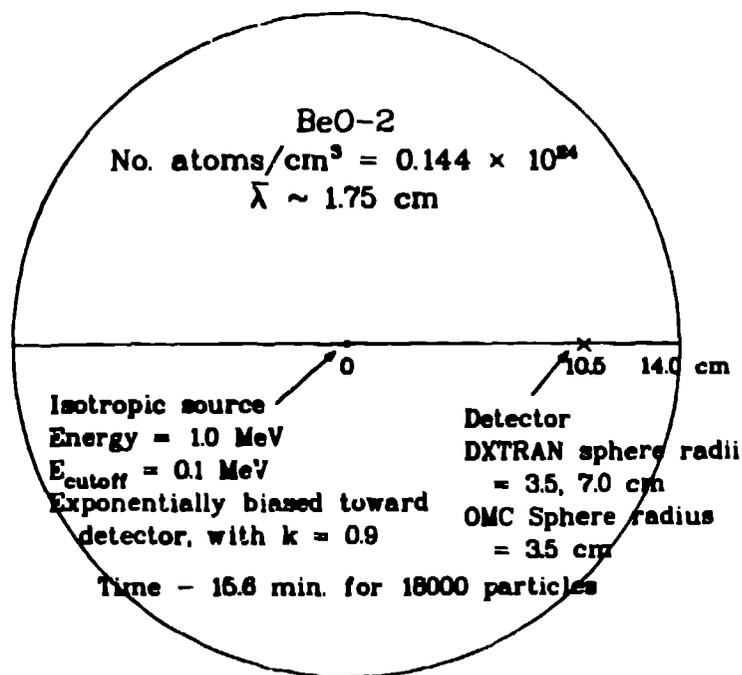
Fig. 11   Geometry for BeO-2 Problem.
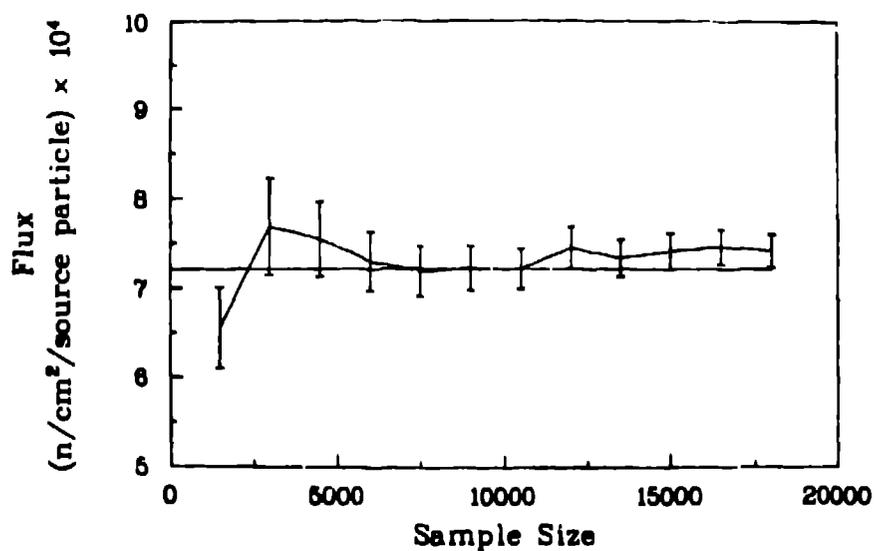


Fig. 12   Flux at a Detector in BeO-2
with the OMCFE and DXTRAN

TABLE I
Comparison of Calculated Flux with Exact Flux

| | Flux (n/cm$^2$/source particle) | | | |
|---|---|---|---|---|
| | Exact (Surface Crossing Estimator) | OMCFE | Ave. Flux (Track Length Estimator) | Error (1 Standard Deviation) |
| Thermal H: Detector 1 | $3.462 \times 10^{-2}$ | $3.486 \times 10^{-2}$ | | $.056 \times 10^{-2}$ |
| Detector 2 | $1.230 \times 10^{-2}$ | $1.231 \times 10^{-2}$ | | $.032 \times 10^{-2}$ |
| Thermal CH$_2$: Detector 1 | $2.086 \times 10^{-1}$ | $2.122 \times 10^{-1}$ | | $.053 \times 10^{-1}$ |
| Detector 2 | $6.259 \times 10^{-2}$ | $6.378 \times 10^{-2}$ | | $.357 \times 10^{-2}$ |
| BeO – 1: Detector 1 | $1.703 \times 10^{-2}$ | $1.697 \times 10^{-2}$ | | $.015 \times 10^{-2}$ |
| Detector 1 | $1.703 \times 10^{-2}$ | | $1.687 \times 10^{-2}$ | $.022 \times 10^{-2}$ |
| BeO – 2: Detector 1 | $7.207 \times 10^{-4}$ | $7.412 \times 10^{-4}$ | | $.185 \times 10^{-4}$ |

In Problem 1 the fluxes at two detector points in thermal H are calculated using the OMCFE. Problem 2 is a similar calculation in thermal $CH_2$. In Problem 3, the flux is calculated at a single detector in a sphere of BeO (non-thermal) for a source of 1 MeV neutrons at the center. The flux is first obtained using the OMCFE, and this is compared with an estimate of the average flux in a sphere about the detector of 1 cm radius. The latter estimate is obtained with the help of DXTRAN. Problem 4 finds the flux at a point in a BeO sphere situated approximately 6 free paths from the source using the OMCFE, but with the aid of a large DXTRAN sphere which encloses the detector. The error-bars (one standard deviation) on the points plotted indicate the statistical accuracy of the calculation in progress, as printed out by the code. The final results are, in every case, within a few percent of the value of the "exact flux" - in fact, the agreement appears somewhat better than expected in at least one case. For example, in the BeO-1 calculation the agreement between the exact flux and that obtained from the average flux in a sphere of 1-cm radius using DXTRAN is surprisingly good. Perhaps that is fortuitous - experience does not lead one to expect it in the average problem. The amount of computing time used could have been reduced in some cases without altering the results appreciably, but in dealing with estimates of flux at a point, it pays to be reasonably cautious. Quite frequently, the calculation is sensitive to the various parameters set in a problem - the size of the imaginary sphere in the OMCFE, the source bias, etc. Some care is essential in setting up a problem and a few short runs can be invaluable in making the necessary decisions, particularly in the case of a difficult problem.

## Concluding Remarks

A very important method of estimating flux at a point in a problem with axial symmetry is through the use of a ring detector. MCNP contains a ring detector option and, although we did not use it in the present calculations, it should be mentioned as one of the tools available.

While the OMCFE in MCNP can deal with neutrons thermalized according to the free gas model, there remains the task of modifying the flux estimator to be compatible with neutrons thermalized with the $S(\alpha,\beta)$ treatment. It is hoped that this defect can be rectified in the not too distant future.

# REFERENCES

1.  H. J. Kalli and E. D. Cashweil, "Evaluation of Three Monte Carlo Estimatior. Schemes for Flux at a Point," Trans. Am. Nucl. Soc. <u>27</u>, 370-371 (Nov. 27—Dec. 2, 1977). Also, Los Alamos Scientific Laboratory Report LA-6865-MS (September, 1977).

2.  M. H. Kalos, "On the Estimation of Flux at a Point by Monte Carlo," Nucl. Sci. Eng. <u>16</u>, 111-117 (1963).

3.  H. A. Steinberg and M. H. Kalos, "Bounded Estimators for Flux at a Point in Monte Carlo," Nucl. Sci. Eng. 44, 406-412 (1971).

4.  H. A. Steinberg, "Bounded Estimation of Flux-at-a-Point for One or More Detectors," Proc. NEACRP Meeting of a Monte Carlo Study Group, Argonne National Laboratory, July 1-3, 1974.

5.  LASL Group X-6, "MCNP - A General Monte Carlo Code for Neutron and Photon Transport," Los Alamos Scientific Laboratory Report LA-7396-M, Revised Manual (November, 1979).